Application of a MILP-based Algorithm for Power Flow Optimisation within More-Electric Aircraft Electrical Power Systems

Xin Wang[(1)], Jason Atkin[(2)], Serhiy Bozhko[(1)], Christopher Hill[(1)]
[(1)]The Department of Electrical and Electronic Engineering, University of Nottingham
[(2)]School of Computer Science, University of Nottingham
[(1)]Aerospace Technology Centre, Innovation Park, Triumph Road, NG7 2TU
[(2)]Computer Science, Jubilee Campus, Wollaton Road, NG8 1BB
Nottingham, United Kingdom
E-Mail: xin.wang2@nottingham.ac.uk

Acknowledgements

This work is funded by the INNOVATIVE doctoral programme. The INNOVATIVE programme is partially funded by the Marie Curie Initial Training Networks (ITN) action, and partially by the Institute for Aerospace Technology (IAT) at the University of Nottingham.

Keywords

« More Electric Aircraft (MEA)», « Electrical Power System (EPS)», « Mixed-Integer Linear Programming (MILP)», « optimal power flow ».

Abstract

This paper presents in detail how Mixed-Integer Linear Programming (MILP) can be used to solve the optimal power flow problem of Electrical Power Systems (EPSs) within More-Electric Aircraft (MEA). Continuous linear functions, integer variables and piecewise-linear functions are modelled to deal with bidirectional power flow, EPS control logic decisions, as well as non-linearity caused by efficiency curves.

Introduction

In recent years, the More Electric Aircraft (MEA) has become a major trend in modern aerospace, aiming for weight reduction and less environmental impact[1]. Many subsystems previously driven by hydraulic, mechanical and pneumatic power have been gradually replaced by electrical systems[2]. As a consequence, the Electrical Power Systems (EPSs) are becoming more and more complex in order to cope with large number of electrical loads. This results in a complicated network with multiple potential power flow options under different flight stages. Power flow optimisation of such a complex network is an important task in order to maximise system efficiency.

The Optimal Power Flow (OPF) problem is large-scale and non-linear containing both continuous and discrete variables, thus it is difficult to solve in real-time[3]. Although some heuristic optimisation algorithms (HOAs) [4] can be adopted, but they can get trapped in a local optimal solution. To avoid this drawback, a practical and beneficial technique Mixed Integer Linear Programming (MILP) can be introduced to solve this problem because of the following advantages:

1) The MILP algorithm can guarantee the optimal solution being the global optimal.
2) Lots of commercial solvers are available to solve MILP problems efficiently with high accuracy, such as, CPLEX, Gurobi, Xpress, etc. In addition, this does not require time and effort to write solution algorithms since the problems can be solved automatically as long as they are specified in the correct MILP format [5][6].

3) Even if HOAs are adopted, it is still worth formulating a MILP model as a benchmark to verify the performance of the applied heuristic method.

Currently, MILP has been widely used in various optimisation problems for terrestrial EPSs. For example, it has been applied to a Unit Commitment (UC) problem to schedule the thermal generators[7][6], and also to solve an optimal sizing problem for integration of renewable energy sources in a micro-grid [8][9][10]. OPF problems formulated by MILP for real-time control have also been proposed in [11][12] for ground based grid applications. However, the EPSs in MEAs have different architectural and operational constraints compared to ground power grids, thus special attentions should be paid to tailor the MILP formulation to the specific OPF problem.

This paper presents in detail how to formulate OPF problems as MILPs which represent the EPSs in MEA in CPLEX. In order to illustrate practical formulation techniques, three major constraints are formulated, focusing on power balance, control logics and bidirectional power flow, as well as cable and non-linear converter efficiency. Three simplified DC EPS topologies shown in the form of power flow diagrams in order to demonstrate the formulations. Based on each topology, the MILP formulation for the OPF problem is provided to demonstrate how to integrate continuous linear functions, integer (or binary) variables and piecewise-linear functions within the problem.

Power balance and continuous linear functions

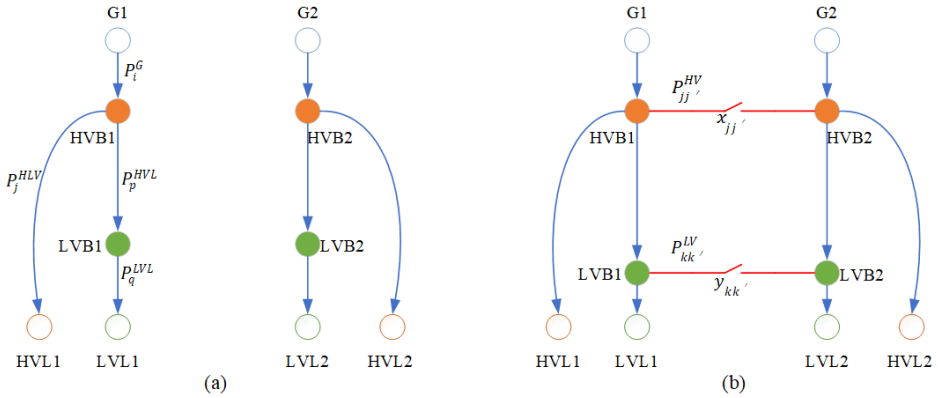

Fig. 1: Simplified power flow diagram of HVDC EPS (a) for basic power flow (b) containing controllable interconnections

In this section, a simplified power flow diagram as shown in Fig.1(a) is taken as an example to demonstrate how the power balance equations are formulated by using Linear Programming (LP). It consists of 2 generator nodes G1 and G2, 2 HVDC bus nodes HVB1 and HVB2, 2 LVDC bus nodes LVB1 and LVB2, 2 HVDC load nodes HVL1 and HVL2, and 2 LVDC load nodes LVL1 and LVL2. The power converters and interconnection between the left-hand and right-hand side are not considered in this section. The power flowing into/out of each node are represented by continuous decision variables. The decision variables used in this section are listed in Table I.

Table I: Notations for the decision variables for power balance

Decision variables	
P_i^G	the power flowing from generator i to the corresponding HV bus
P_j^{HLV}	the power flowing from HV bus j to LV bus j
P_p^{HVL}	the power drawn from HV bus by HV load p
P_q^{LVL}	the power drawn from LV bus by LV load q

Objective function

The objective is to minimise the total electrical power production of the generators and the objective function is expressed in (1), where N^G is the number of generators. The same objective function is also applicable for section 3 and 4.

$$f = f_G = \frac{1}{N^G}\sum_i P_i^G \tag{1}$$

Constraints

1. Power balance constraints

Power balance for each node is an essential constraint in optimal power flow formulation in order to maintain voltage stability. The power flowing through each node should strictly comply with the rule that the sum of power flowing into/out of each node equals zero. For all HV/LV bus nodes, the power balance equations are presented in (2) and (3), where N^{HVB} and N^{HLB} are the number of HV and LV buses, respectively. The left side represents the input power, while the right side represents the output power.

$$P_j^G = P_j^{HLV} + P_j^{HVL}, \forall j \in \{1, \dots, N^{HVB}\} \tag{2}$$

$$P_k^{HLV} = P_k^{LVL}, \forall k \in \{1, \dots, N^{LVB}\} \tag{3}$$

2. Power limitation constraints

In the EPS, each component or connection has a capacity limitation. In this case, power produced by the generators could not exceed their capacities $P_{i\_max}^G$. And all power flow variables are defined non-negative values.

$$0 \le P_i^G \le P_{i\_max}^G \tag{4}$$

$$0 \le P_j^{HLV}, P_p^{HVL}, P_q^{LVL} \tag{5}$$

Control logic and binary variables

In this section, the controllable interconnections between HV/LV buses are added to the basic power flow balance case to consider a wider range of power routing options. The adapted power flow diagram is shown in Fig.1(b). Therefore, new decision variables should be introduced to present the contactor connection status – on/off. These can be appropriately represented by binary variables.

The HV/LV bus interconnections provide bidirectional power flow into this case. For some elements of the model (e.g. where cable losses depend upon power flow) the scalar value of power flow is needed. For this reason, the power flow is represented by two non-negative variables, one for the power flow in each direction. Two binary variables, one for each direction, are also used to indicate whether power can flow in that direction. The notations of new decision variables are listed in Table II.

Table II: Notations for the decision variables for power balance

Decision variables	
$f_{jj'}^{HV} \in \{0,1\}$	the indicator variables for power flow direction from HV bus j to HV bus j'
$f_{kk'}^{HV} \in \{0,1\}$	the indicator variable for power flow direction from LV bus k to LV bus k'
$x_{jj'} \in \{0,1\}$	the contactor status between HV bus j and HV bus j'
$y_{kk'} \in \{0,1\}$	the contactor status between LV bus k and LV bus k'
$P_{jj'}^{HV}$	the power flow from HV bus j to HV bus j'
$P_{kk'}^{LV}$	the power flow from LV bus k to LV bus k'

1. Modified power balance constraints

The power balance equations for HV and LV bus nodes are modified accordingly, and they are given in (6) and (7). For HV bus power balance equations, either $\sum_{j\neq j'} P_{j'j}^{HV}$ or $\sum_{j\neq j'} P_{jj'}^{HV}$ is 0, and similarly for LV bus, either $\sum_{k\neq k'} P_{k'k}^{LV}$ or $\sum_{k\neq k'} P_{kk'}^{LV}$ is 0, which will be presented in the unidirectional constraints.

$$P_j^G + \sum_{j\neq j'} P_{j'j}^{HV} = P_j^{HVL} + P_j^{HLV} + \sum_{j\neq j'} P_{jj'}^{HV}, \forall j \in \{1, \dots, N^{HVB}\} \quad (6)$$

$$P_k^{HLV} + \sum_{k\neq k'} P_{k'k}^{LV} = P_k^{LVL} + \sum_{k\neq k'} P_{kk'}^{LV}, \forall k \in \{1, \dots, N^{LVB}\} \quad (7)$$

2. Contactor connection constraints

The power contactor between HV buses is allowed to be closed only if there are generator failures. To consider a wider range of options, LV buses are allowed to be closed freely no matter the existence of generator failures, despite the fact that this is unlikely in practice. The contactor connection constraints can be listed as follows in (8) - (10), where α_i is the connection status of the generators; $P_{jj'\_max}^{HV}$ and $P_{kk'\_max}^{LV}$ are maximum power can be transferred between HV/LV buses. The HV bus interconnection constraints are represented by (8), as well as the power exchange constraints between buses given by (9) and (10), which indicate the power flows are forced to be 0 when the binary indicator variables are 0.

$$x_{jj'} + \sum_i \alpha_i \leq N^G \quad (8)$$

$$0 \leq P_{jj'}^{HV} \leq f_{jj'}^{HV} P_{jj'\_max}^{HV} \quad (9)$$

$$0 \leq P_{kk'}^{LV} \leq f_{kk'}^{LV} P_{kk'\_max}^{LV} \quad (10)$$

3. Unidirectional constraints

Power exchange between the HV/LV buses is bidirectional, but it cannot flow in both directions simultaneously. For example, for HV buses, if $P_{jj'}^{HV} > 0$ the power flow form node *j* to node *j'*, then $P'^{HV}_{jj'} = 0$. The binary power indicators could be 0 or 1, if power flows from j to j', then $f_{jj'}^{HV} = 1$, and the other direction is forced to be 0. If the connector is open, then both variables are forced to 0. This *if…then…* function can be realized when the constraints in (11) - (12) are combined with those in (9) - (10).

$$f_{jj'}^{HV} + f_{j'j}^{HV} = x_{jj'} \quad (11)$$

$$f_{kk'}^{LV} + f_{k'k}^{LV} = y_{kk'} \quad (12)$$

Component efficiency and linearization

In this section, the EPS system is modelled more precisely by considering the cable losses and converter efficiencies. The power flow diagram adopted in this section is shown in Fig. 1. Two power converters are added and represented by nodes Con1 and Con2.

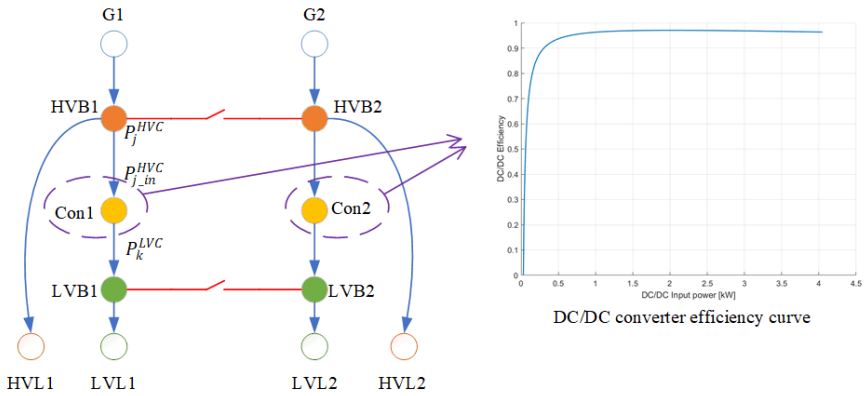

Fig. 1 Simplified power flow diagram of HVDC EPS containing power converters with a typical efficiency curve

To simplify the model, cable losses are assumed to be a linear function of the power flowing through it. But for the DC/DC converters, a typical nonlinear relationship between input power and efficiency is utilised, as shown in Fig. 1. It results in a nonlinear problem unsuitable to MILP, therefore a piecewise function is adopted to linearize this nonlinear relationship and the newly introduced notations are listed in Table III.

Table III Notations of added parameters and decision variables for cables and converters

Parameters	
P_{max}^{C}	the capacity of DC-DC converter
η_c	the efficiency of DC/DC converter
$\eta_{jj'}^{HV}$	the cable efficiency of HV bus connection between bus j and j' assuming constant
$\eta_{kk'}^{LV}$	the cable efficiency of LV bus connection between bus k and k' assuming constant
η_j^{HVC}	the cable efficiency between the HV bus j and the connected converter assuming constant
η_k^{LVC}	the cable efficiency between the LV bus k and the connected converter assuming constant
Decision variables	
P_j^{HVC}	the power flowing from HV bus j to the connected DC/DC converter
$P_{j\_in}^{HVC}$	the power flow injected to the DC/DC converter from the corresponding HV bus j
P_k^{LVC}	the power flowing from DC/DC converter to LV bus k

1. Modified power balance constraints

For all HV/LV bus nodes, the power balance equations considering efficiencies are presented in (13) and (14).

$$P_j^G + \sum_{j\neq j'} \eta_{jj'}^{HV} P_{j'j}^{HV} = P_j^{HVC} + P_j^{HVL} + \sum_{j\neq j'} P_{jj'}^{HV}, \forall j \in \{1,\dots,N^{HVB}\} \quad (13)$$

$$\eta_k^{LVC} P_k^{LVC} + \sum_{k\neq k'} \eta_{kk'}^{LV} P_{k'k}^{LV} = P_k^{LVL} + \sum_{k\neq k'} P_{kk'}^{LV}, \forall k \in \{1,\dots,N^{LVB}\} \quad (14)$$

For all converter nodes, the power balance equation is presented in (15), where N^C is the number of converters, and $P_{c\_in}^{HVC} = \eta_c^{HVC} P_c^{HVC}$.

$$\eta_c P_{c\_in}^{HVC} = P_c^{LVC}, \forall c \in \{1,\dots,N^C\} \quad (15)$$

2. Linear approximation in constraints

In (15), the efficiency of converter has nonlinear relationship to $P_{c\_in}^{HVC}$ as illustrated in Fig. 1, which can be represented as $\eta_c = f_\eta(P_{c\_in}^{HVC})$. Therefor it can be presented in the format of (16) resulting to the nonlinearity.

$$f_\eta(P_{c\_in}^{HVC})P_{c\_in}^{HVC} - P_c^{LVC} = 0 \tag{16}$$

In this case, a new decision variable $P_{c\_out}^{HVC}$ is introduced to represent the converter's output power. The output power of the converter could be approximated by a piecewise function of its input power, and each segment is a linear function relating to the input power as demonstrated in (17). Such that the optimal problem can then be formulised as a MILP.

$$P_{c\_out}^{HVC} = \eta_c P_{c\_in}^{HVC} \approx f_p(P_{c\_in}^{HVC}) = \begin{cases} k_1 P_{c\_in}^{HVC} + b_1 \ (m_0 \le P_{c\_in}^{HVC} \le m_1) \\ k_2 P_{c\_in}^{HVC} + b_2 \ (m_1 \le P_{c\_in}^{HVC} \le m_2) \\ k_3 P_{c\_in}^{HVC} + b_3 \ (m_2 \le P_{c\_in}^{HVC} \le m_3) \\ \vdots \\ k_n P_{c\_in}^{HVC} + b_n \ (m_{n-1} \le P_{c\_in}^{HVC} \le m_n) \end{cases} \tag{17}$$

$$\widetilde{\eta_c} = \frac{k_m P_{c\_in}^{HVC} + b_m}{P_{c\_in}^{HVC}} = k_m + \frac{b_m}{P_{c\_in}^{HVC}} \tag{18}$$

Taking the typical efficiency curve in Fig. 2(a) as an example, the corresponding output power $P_{c\_out}^{HVC}$ can be illustrated in relationship to the input power $P_{c\_in}^{HVC}$ in blue, while the piecewise linear approximation of $P_{c\_out}^{HVC}$ is in red with 5 segments. The approximated output power curve matches very well with the output power based on typical efficiency curves. To verify the accuracy of the approximation, the approximated converter efficiency $\widetilde{\eta_c}$ can be derived in (18), and the curves are compared in Fig. 2(b). The figure shows that the approximated efficiency $\widetilde{\eta_c}$ is very close to the typical efficiency curve.

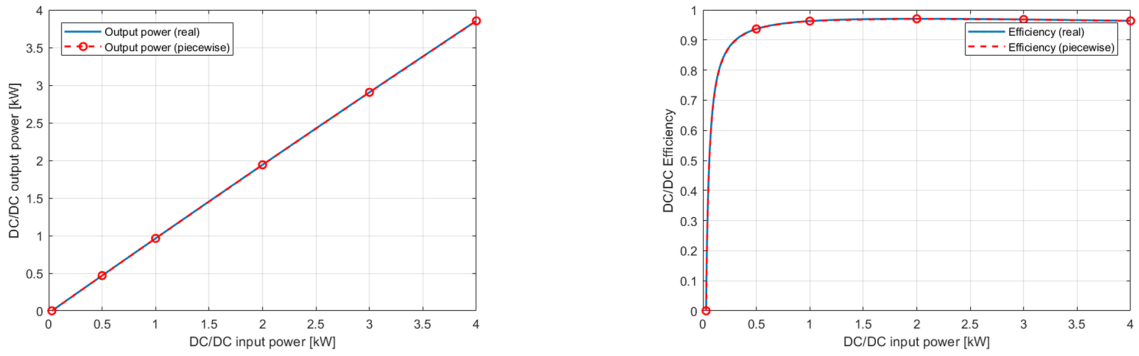

(a) (b)

Fig. 2 Piecewise curves (a) Piecewise output power curve compared to the output power based on typical efficiency curve (b) The piecewise function derived efficiency curve compared to the typical efficiency curve

Case study of one generator failure

To verify the effectiveness of the proposed model and algorithms, a case study of one generator failure is presented in this section base on the topology in Fig. 3. The optimal solution should decide HV/LV bus connections and the power flowing into/out of each component.

According to the predefined parameters, the HV buses should be connected together due to the generator failure, and the two converters should have the same power flow because of the same LV loads. The simulation results solved by CPLEX are given in Fig. 3, and the converter efficiency derived in this case is marked on the efficiency curve. It shows that the power balance is realized for all the nodes and connections considering the efficiencies. The HV buses are automatically connected together to transfer the power from the working generator. This corresponds to the previous analysis, hence the effectiveness for the model formulation for solving binary decision variables has been verified. Furthermore, the two converters transfer balanced power to the two equal LV loads, and have the same piecewise function derived efficiency located on the real efficiency curve. Thus, it proves that the piecewise function is sufficiently accurate to deal with the non-linearity.
This sentence will be repeated to represent the body of the text. This is where you continue to write the extended paper, including subparagraphs, sub-sub paragraphs, figures, formulae, tables and eventual images.

Cable efficiencies	
Parameters	Values
$\eta_{jj'}^{HV}$	0.9998
$\eta_{kk'}^{LV}$	0.8000
η_{j}^{HVC}	0.9996
η_{k}^{LVC}	0.9996
Load requirements (kW)	
P_{p}^{HVL}	{40, 20}
P_{q}^{LVL}	{2, 2}

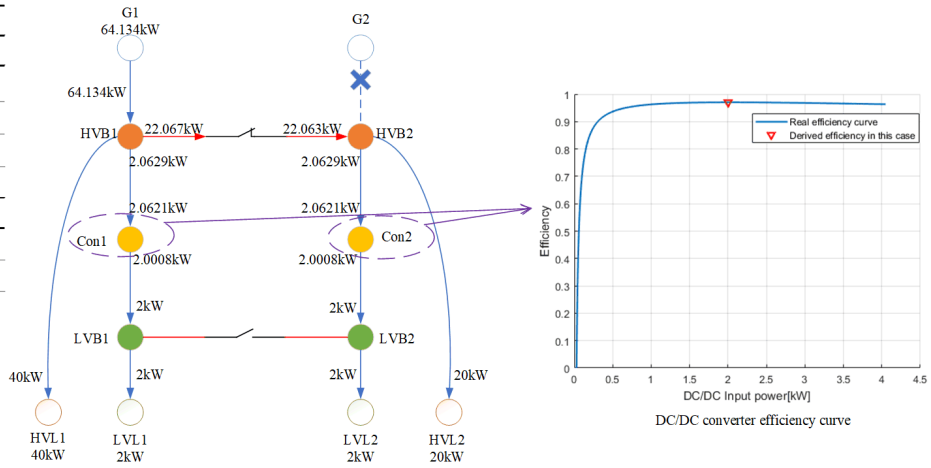

Fig. 3 Optimal power flow in the defined case

Conclusion

This paper gives a detailed introduction of how to apply MILP to OPF problems which represent EPSs in MEA. Complex OPF problems were divided into three topics – power balance, control logic of the contactors, and components efficiency (including non-linear converter efficiency). For each topic, this paper adopted simplified EPS topologies which aimed to present clearly how to integrate continuous linear functions, integer (or binary) variables and piecewise-linear functions into the problem. The effectiveness of the proposed model and algorithms has been verified in a case study solved by using CPLEX. The modelling methods presented in this paper could be extended to other complex and large-scale OPF problems which contain nonlinearities: this is a topic of our current studies and the results will be reported in the following publications.

References

[1] F. Gao, S. Bozhko, A. Costabeber, G. Asher, and P. Wheeler, “Control Design and Voltage Stability Analysis of a Droop-Controlled Electrical Power System for More Electric Aircraft,” IEEE Trans. Ind. Electron., vol. 64, no. 12, pp. 9271–9281, 2017.

[2] P. Wheeler and S. Bozhko, “The More Electric Aircraft,” IEEE Electrif. Mag., no. December, pp. 1–7, 2014.

[3] S. Lin and Y. Ho, “An Ordinal Optimization Theory Based Algorithm for Solving the Optimal Power Flow Problem With Discrete Control Variables,” IEEE Trans. Power Syst., vol. 19, no. 1, pp. 276–286, 2004.

[4] M. Niu, C. Wan, and Z. Xu, “A review on applications of heuristic optimization algorithms for optimal power flow in modern power systems,” J. Mod. Power Syst. Clean Energy, vol. 2, no. 4, pp. 289–297, 2014.

[5] L. M. Hvattum, A. Løkketangen, and F. Glover, “Comparisons of Commercial MIP Solvers and an Adaptive Memory (Tabu Search) Procedure for a Class of 0-1 Integer Programming Problems,” Algorithmic Oper. Res., vol. 7, no. 1, pp. 13–20, 2012.

[6] A. Viswanath, L. Goel, and P. Wang, “Mixed integer programming formulation techniques and applications to Unit Commitment problem,” 10th Int. Power Energy Conf. IPEC 2012, pp. 25–30, 2012.

[7] V. K. Tumuluru, Z. Huang, and D. H. K. Tsang, “Unit commitment problem: A new formulation and solution method,” Int. J. Electr. Power Energy Syst., vol. 57, pp. 222–231, 2014.

[8] L. K. Gan, J. K. H. Shek, and M. a. Mueller, “Optimisation Sizing of Hybrid Wind-Diesel Systems using Linear Programming Technique,” 7th IET Int. Conf. Power Electron. Mach. Drives (PEMD 2014), p. 4.1.04-4.1.04, 2014.

[9] A. Scalfati, D. Iannuzzi, M. Fantauzzi, and M. Roscia, “Optimal sizing of distributed energy resources in smart microgrids: A mixed integer linear programming formulation,” 2017 6th Int. Conf. Renew. Energy Res. Appl. ICRERA 2017, vol. 2017–Janua, pp. 568–573, 2017.

[10] S. X. Chen, H. B. Gooi, and M. Q. Wang, “Sizing of energy storage for microgrids,” IEEE Trans. Smart Grid, vol. 3, no. 1, pp. 142–151, 2012.

[11] A. Yoza, K. Uchida, A. Yona, and T. Senju, “Optimal operation method of smart house by controllable loads based on smart grid topology,” Int. J. Emerg. Electr. Power Syst., vol. 14, no. 5, pp. 411–420, 2013.

[12] C. Shao, X. Wang, M. Shahidehpour, X. Wang, and B. Wang, “An MILP-Based Optimal Power Flow in Multicarrier Energy Systems,” IEEE Trans. Sustain. Energy, vol. 8, no. 1, pp. 239–248, 2017